Inorganic Chemistry

Article

pubs.acs.org/IC

Thermally Induced Defluorination during a *mer* to *fac* Transformation of a Blue-Green Phosphorescent Cyclometalated Iridium(III) Complex

Yonghao Zheng, Andrei S. Batsanov, Robert M. Edkins, Andrew Beeby, and Martin R. Bryce*

Department of Chemistry, Durham University, Durham DH1 3LE, U.K.

Supporting Information

ABSTRACT: The new homoleptic tris-cyclometalated [Ir(C^N)$_3$] complexes *mer*-**8**, *fac*-**8**, and *fac*-**9** incorporating γ-carboline ligands are reported. Reaction of 3-(2,4-difluorophenyl)-5-(2-ethylhexyl)-pyrido[4,3-*b*]indole **6** with iridium(III) chloride under standard cyclometalating conditions gave the homoleptic complex *mer*-**8** in 63% yield. The X-ray crystal structure of *mer*-**8** is described. The Ir−C and Ir−N bonds show the expected bond length alternations for the differing *trans* influence of phenyl and pyridyl ligands. *mer*-**8** quantitatively isomerized to *fac*-**8** upon irradiation with UV light. However, heating *mer*-**8** at 290 °C in glycerol led to an unusual regioselective loss of one fluorine atom from each of the ligands, yielding *fac*-**9** in 58% yield. *fac*-**8** is thermally very stable: no decomposition was observed when *fac*-**8** was heated in glycerol at 290 °C for 48 h. The γ-carboline system of *fac*-**8** enhances thermal stability compared to the pyridyl analogue *fac*-Ir(46dfppy)$_3$ **10**, which decomposes extensively upon being heated in glycerol at 290 °C for 2 h. Complexes *mer*-**8**, *fac*-**8**, and *fac*-**9** are emitters of blue-green light (λ_{max}^{em} = 477, 476, and 494 nm, respectively). The triplet lifetimes for *fac*-**8** and *fac*-**9** are ∼4.5 μs at room temperature; solution Φ_{PL} values are 0.31 and 0.22, respectively.

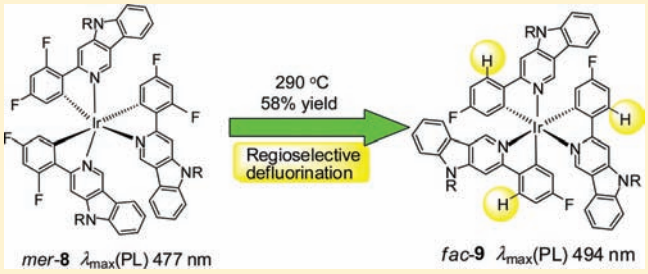

INTRODUCTION

Luminescent transition metal complexes are employed in a diverse range of applications, notably as phosphorescent emitters for organic light-emitting displays (OLEDs)[1−6] and for solid-state lighting.[7] In this regard, cyclometalated iridium(III) complexes have received special attention as dopants for harvesting the otherwise nonemissive triplet states formed in OLEDs.[8−10] The complexes are charge neutral and generally have good chemical and photochemical stability, combined with highly efficient emission from triplet metal-to-ligand charge-transfer (MLCT) states. Tris-homoleptic Ir(III) complexes [Ir(C^N)$_3$], where C^N is a monoanionic bidentate ligand [e.g., 2-phenylpyridine (ppy)], have been extensively studied. Two stereoisomers can occur, designated *facial* (*fac*) and *meridional* (*mer*). The *fac* and *mer* isomers are the thermodynamically and kinetically controlled products, respectively. Generally, the *mer* isomer has a red-shifted emission, a significantly decreased quantum efficiency, and a shorter emission lifetime compared to those of the *fac* isomer, all of which are considered undesirable. The *mer* isomers are not widely studied: they can usually be isomerized to the *fac* isomer thermally (above ∼200 °C) or by irradiation with UV light.[11−15]

The HOMO of Ir(III) complexes consists principally of a mixture of phenyl π-orbitals and Ir d-orbitals, whereas the LUMO is predominantly located on ppy, especially the pyridyl π-orbitals. Structural changes in the skeletal and substituent groups of the cyclometalating ligand lead to color tuning of phosphorescence.[16−20] For example, the attachment of electron-withdrawing substituents, notably fluorine, to the phenyl ring of ppy ligands is an established strategy for hypsochromically shifting the emission by lowering the HOMO energy, resulting in an increased HOMO−LUMO gap.[21−27] Electron-donating groups on the phenyl ring and electron-withdrawing groups on the pyridyl moiety, or an extended ligand chromophore, bathochromically shift the emission.[28] Efficient blue emitters remain challenging targets.

Studies on carbazolyl-Ir derivatives are very limited. Our group[29,30] and Ho et al.[31] have recently established that *fac*-Ir(III) complexes of 3-pyridylcarbazole ligands, e.g., **1** (Chart 1), are emitters of green light with good stability and high photoluminescence quantum yields. We sought to explore new analogues, and TD-DFT calculations (B3LYP/3-21G*/LANL2DZ level) were used to guide the choice of molecules for synthesis. We were attracted to the 2-phenyl-γ-carboline system **2**, which is isomeric with **1**, for the following reasons. (i) The TD-DFT calculations suggested that the $T_1 \leftarrow S_0$ transition of **2** (2.53 eV) is similar in energy to that of **1** (2.63 eV) and should, therefore, retain the green emission observed for **1**,[29−31] whereas for isomeric systems, the comparable transitions are lower in energy (see Chart 2 and Results and Discussion). (ii) System **2** is synthetically accessible in a few steps, and functionalization of the cyclometalated

Received: August 1, 2011
Published: December 19, 2011

   dx.doi.org/10.1021/ic201655n | *Inorg. Chem.* 2012, 51, 290−297

Chart 1. Structures of Complexes 1, 2, and 8−10

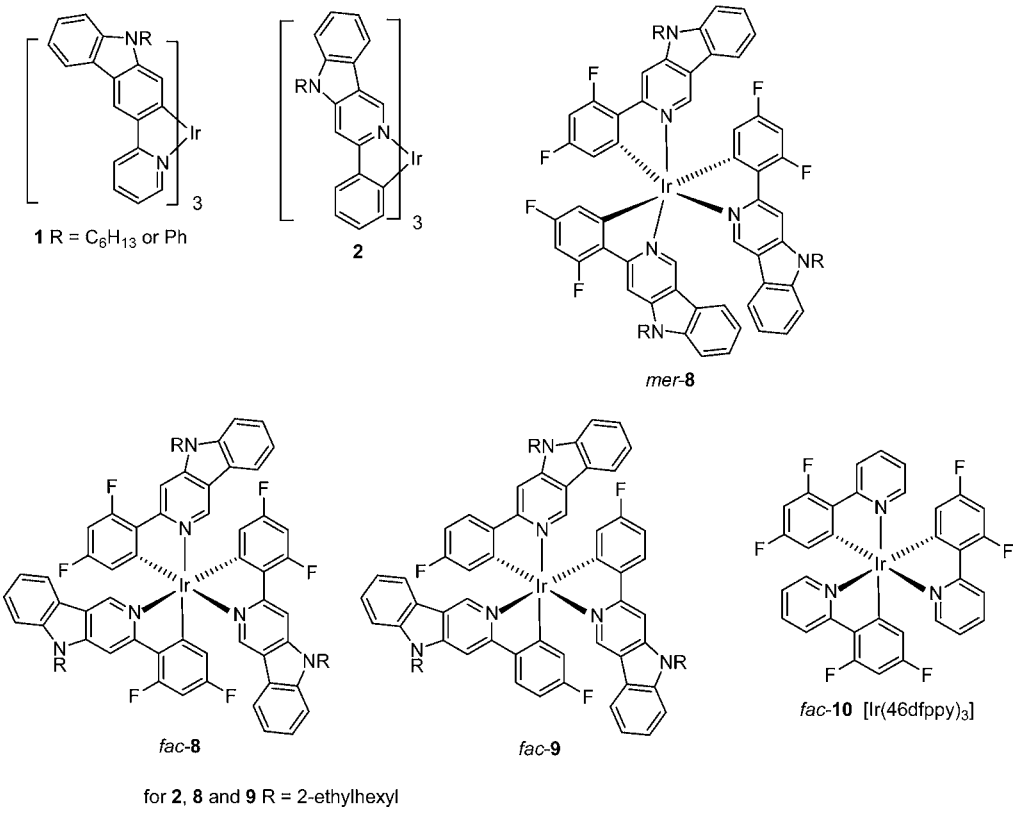

Chart 2. Structures of the Parent Isomeric Complexes Used in the DFT Calculations

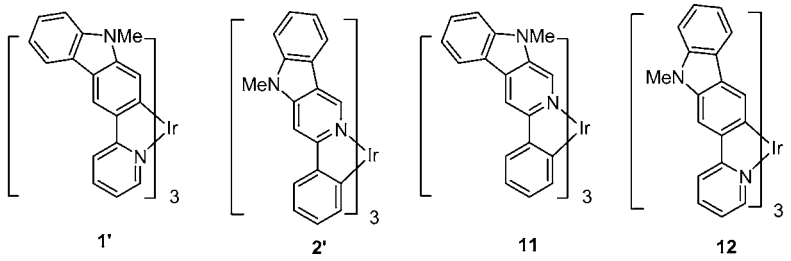

phenyl ring of **2** should allow the emission color to be tuned by analogy with ppy analogues discussed above.

In this Article, we focus on complexes **8** and **9**, which are derivatives of **2** with fluorinated phenyl rings. The following findings are the most interesting aspects of this work. (i) *mer*-**8** can be cleanly converted into *fac*-**8** photochemically, but not thermally. (ii) Under thermal conditions, *mer*-**8** undergoes regioselective loss of one fluorine atom from each ligand to yield *fac*-**9** in good yield. (iii) The complexes are efficient emitters of blue-green light. (iv) Improved thermal stability is imparted by the γ-carboline moiety of *fac*-**8**, compared to the pyridyl analogue, *fac*-Ir(46dfppy)$_3$ **10**.

EXPERIMENTAL SECTION

Materials, Synthesis, and Characterization. All reactions were conducted under a blanket of argon that was dried by being passed through a column of phosphorus pentoxide. All commercial chemicals were used without further purification unless otherwise stated. Solvents were dried through an HPLC column on an Innovative Technology Inc. solvent purification system. Column chromatography was conducted using 40−60 μm mesh silica. NMR spectra were recorded on Bruker Avance 400 MHz or Varian VNMRS 500, 600, and 700 MHz spectrometers. Chemical shifts are referenced to tetramethylsilane [Si(CH$_3$)$_4$] at 0.00 ppm. Melting points were determined in open-ended capillaries using a Stuart Scientific SMP3 melting point apparatus at a ramping rate of 5 °C/min and are uncorrected. Mass spectra were recorded on a Waters Xevo OTofMS instrument with an ASAP probe, a Thermoquest Trace instrument, or a Thermo-Finnigan DSQ instrument. Elemental analyses were performed on a CE-400 elemental analyzer. Cyclic voltammograms were recorded at a scan rate of 100 mV/s at room temperature using an airtight single-compartment three-electrode cell equipped with a Pt disk working electrode, a Pt wire counter electrode, and a Pt wire pseudoreference electrode. The cell was connected to a computer-controlled Autolab PG-STAT 30 potentiostat. The solutions contained the complex and *n*-Bu$_4$NPF$_6$ (0.1 M) as the supporting electrolyte in dichloromethane. All potentials are reported with reference to an internal standard of the decamethylferrocene/decamethylferrocenium couple ($FcMe_{10}/FcMe_{10}^+$ = 0.00 V).

Absorption spectra were recorded using a Unicam UV2-100 spectrometer operated with Unicam Vision in 1 cm path-length quartz cells. Excitation and emission photoluminescence spectra were recorded on a Horiba Jobin Yvon SPEX Fluorolog FL3-22 spectrofluorometer. Samples were held in quartz fluorescence cuvettes (l = 1 cm × 1 cm) and degassed by repeated freeze−pump−thaw cycles. Solutions had A values of 0.10−0.15 at 400 nm to minimize

dx.doi.org/10.1021/ic201655n | Inorg. Chem. 2012, 51, 290−297

Scheme 1. Synthesis of *mer*-8, *fac*-8, and *fac*-9[a]

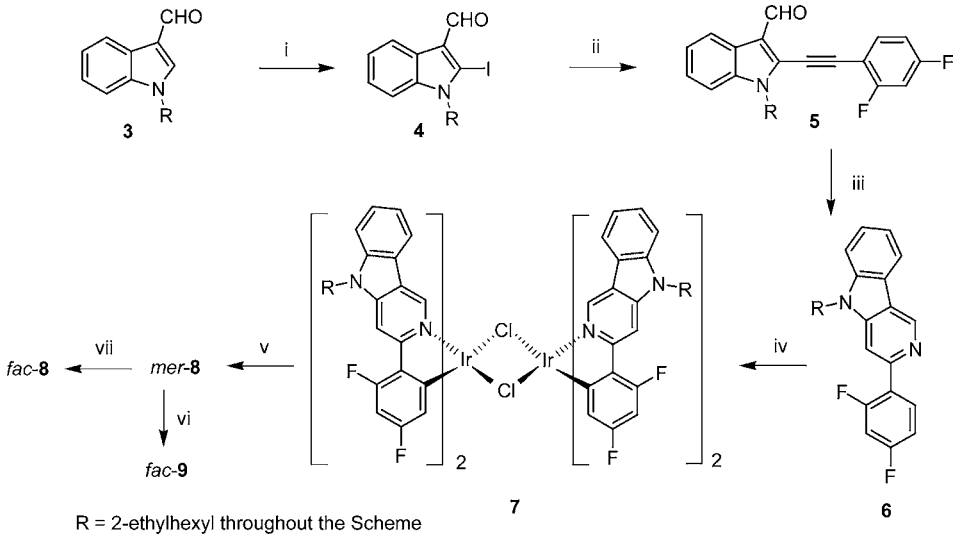

[a]Reagents and conditions: (i) I_2, *N*-methylpiperazine, *n*-BuLi, THF, −78 to −23 °C, 60% yield; (ii) 2,4-difluorophenylacetylene, $Pd(PPh_3)_4$, CuI, NEt_3, 20 °C, 90% yield; (iii) *t*-$BuNH_2$, toluene, 100 °C, 60% yield; (iv) $IrCl_3{\cdot}3H_2O$, 2-ethoxyethanol, water, 120 °C; (v) **6**, ethylene glycol, acetylacetone, NEt_3, 190 °C, ∼62% yield for step iv, based on $IrCl_3{\cdot}3H_2O$, ∼63% for step v, based on **7**; (vi) glycerol, 290 °C, 58% yield; (vii) *hν* (365 nm), CD_2Cl_2, 100% yield.

inner filter effects. PLQYs were measured using the integrating sphere technique.[32] For photoluminescence lifetime measurements, samples were prepared and degassed in the same way as described for steady-state photoluminescence measurements. In a homemade setup, a N_2 laser (337 nm, 10 μJ, 10 Hz) was used as an excitation source. Emission was detected in a 90° geometry by a photomultiplier tube (Hamamatsu R928) as a function of time, selecting a wavelength close to the peak emission by way of a monochromator (Horiba Jobin Yvon Triax 320) with a 0.1−2.0 nm bandpass. The signal was averaged and converted to a digital signal by a digital storage oscilloscope (Tetronix TDS 340). The data were fitted to single-exponential functions of the form $I(t) = I_0 \exp(-t/\tau)$.

Complex *mer*-8. A mixture of **6** (0.60 g, 1.5 mmol), iridium chloride trihydrate (0.24 g, 0.67 mmol), and 2-ethoxyethanol and water [10 mL, 3:1 (v/v)] was stirred at 120 °C overnight. The precipitate was collected by suction filtration, and the intermediate yellow solid **7** was dried (0.42 g, ∼62% based on $IrCl_3{\cdot}3H_2O$). Anal. Calcd for $C_{100}H_{100}N_8F_8Cl_2Ir_2$: C, 59.42; H, 4.99; N, 5.54. Found: C, 59.18; H, 5.11; N, 5.35. ^{1}H NMR (600 MHz, $CDCl_3$): δ 9.74 (4H, s), 8.11 (4H, s), 7.36−7.26 (4H, m), 7.22 (4H, m), 7.07 (4H, m), 6.91−6.73 (4H, m), 6.37−6.11 (4H, m), 5.29−5.13 (4H, m), 3.91−3.67 (4H, m), 3.51 (4H, m), 1.79 (4H, m), 1.40−1.10 (32H, m), 0.99−0.57 (24H, m). ^{19}F NMR (564 MHz, $CDCl_3$): δ −110.05 to −110.86 (4F, m), −112.08 (4F, dd, *J* = 27.9, 15.5 Hz). MS (MALDI+): *m*/*z* 2020.8 (M+, 100%). A mixture of **6** (0.12 g, 3.1 mmol), **7** (0.15 g, 0.07 mmol), ethylene glycol (10 mL), acetylacetone (0.1 mL), and NEt_3 (0.1 mL) was stirred at 190 °C overnight. The precipitate was collected by suction filtration. The crude product was purified by column chromatography [SiO_2, 2:3 (v/v) DCM/hexane eluent], yielding *mer*-**8** (0.12 g, ∼63% based on **7**) as a yellow solid. Crystals for X-ray analysis were grown by slow cooling of a solution of *mer*-**8** in DCM and hexane [1:2 (v/v)]. Anal. Calcd for $C_{75}H_{75}F_6IrN_6$: C, 65.91; H, 5.53; N, 6.15. Found: C, 66.11; H, 5.63; N, 5.98. ^{1}H NMR (500 MHz, $CDCl_3$): δ 8.74 (1H, t, *J* = 3.0 Hz), 8.68 (1H, d, *J* = 7.4 Hz), 8.41 (1H, s), 8.28 (2H, s), 8.16 (1H, s), 7.83 (1H, t, *J* = 7.1 Hz), 7.79−7.71 (1H, m), 7.54−7.33 (8H, m), 7.23 (1H, dd, *J* = 14.2, 6.7 Hz), 7.03 (1H, t, *J* = 7.6 Hz), 6.63 (1H, s), 6.53 (2H, dd, *J* = 22.8, 13.0 Hz), 6.48−6.40 (1H, m), 6.09 (1H, t, *J* = 7.3 Hz), 5.94−5.80 (1H, m), 4.29−4.08 (6H, m), 2.07 (3H, d, *J* = 8.9 Hz), 1.50−1.13 (24H, m), 1.07−0.78 (18H, m). ^{19}F NMR (470 MHz, $CDCl_3$): δ −110.59 (1F, br) −111.06 (1F, dd, *J* = 15.8, 7.5 Hz), −111.26 (1F, br) −111.50 (2F, m), −112.84 (1F, br). HRMS (FTMS + ESI): calcd for $C_{75}H_{75}F_6{}^{193}IrN_6$ 1366.5587, found 1366.5579.

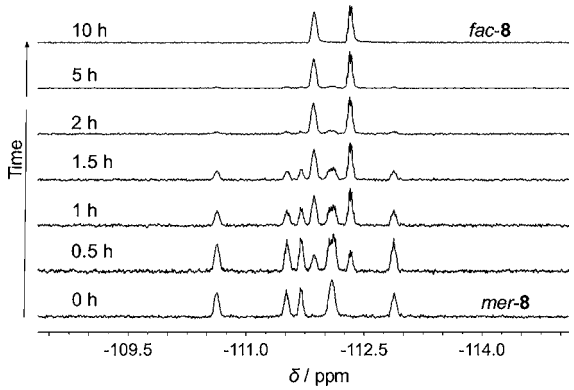

Figure 1. ^{19}F NMR spectroscopic monitoring of the photochemical conversion of *mer*-**8** to *fac*-**8**.

The single-crystal diffraction experiment was conducted on a three-circle Bruker diffractometer with a SMART 6000 CCD area detector, using graphite-monochromated Mo Kα radiation (λ = 0.71073 Å) and Cryostream 700 (Oxford Cryosystems) open-flow N_2 cryostats. Crystal data: $C_{75}H_{75}IrF_6N_6{\cdot}xC_6H_{14}$ (tentatively $x \approx {}^1/_2$), *M* = 1409.7, *T* = 120 K, triclinic, space group $P\bar{1}$ (No. 2), *a* = 12.329(1) Å, *b* = 15.423(1) Å, *c* = 18.341(2) Å, α = 106.96(1)°, β = 95.64(1)°, γ = 91.03(1)°, *V* = 3315.6(5) Å^3, *Z* = 2, D_c = 1.412 g/cm^3, μ = 2.08 mm^{-1}, 32728 reflections with $2\theta \leq 50°$, 11671 unique reflections, R_{int} = 0.081, R_1 = 0.049 [8266 data with $I \geq 2\sigma(I)$], $wR_2(F^2)$ = 0.117 (all data). The structure was determined by Patterson methods and refined by full-matrix least-squares against F^2 of all data, using SHELXTL version 6.12[33] and OLEX2.[34] Structural data in CIF format is available as Supporting Information or from the Cambridge Structural Database (CCDC-835332).

Complex *fac*-8. *mer*-**8** (4.3 mg, 3.1 μmol) was dissolved in CD_2Cl_2 (0.5 mL) in a Young's tap NMR tube and degassed three times by freeze−pump−thaw cycles. The sample was irradiated by two LEDs at 365 nm (∼100 mW each) positioned 2 cm from the sample for a total period of 10 h with intermittent agitation. The conversion

dx.doi.org/10.1021/ic201655n | *Inorg. Chem.* 2012, 51, 290−297

was monitored by ^{19}F NMR until the isomerization to *fac*-**8** was judged to have reached completion (100% yield by NMR). A yellow solid was obtained by removing the solvent. Anal. Calcd for $C_{75}H_{75}F_6IrN_6 \cdot CH_2Cl_2$: C, 62.87; H, 5.35; N, 5.79. Found: C, 62.83; H, 5.80; N, 5.43. ^1H NMR (700 MHz, CD_2Cl_2): δ 8.43 (3H, d, J = 3.5 Hz), 8.21 (3H, m), 7.50 (3H, m), 7.45 (6H, m), 7.05 (3H, m), 6.40 (6H, m), 4.27 (6H, m), 2.13 (3H, m), 1.52−1.24 (24H, m), 0.99 (9H, dt, J = 28.4, 7.4 Hz), 0.88 (9H, dt, J = 24.9, 7.3 Hz). ^{19}F NMR (658 MHz, CD_2Cl_2): δ −111.51 (3F, m), −111.95 (3F, quintet, J = 6.6 Hz). HRMS (MS AP+): calcd for $[C_{75}H_{75}F_6{}^{193}IrN_6]$ 1366.5587, found 1366.5583.

Complex *fac*-9. A mixture of *mer*-**8** (0.06 g, 0.04 mmol) and glycerol (10 mL) was stirred at 290 °C for 72 h. The residue was extracted with dichloromethane (3 × 10 mL). The organic layers were combined, dried ($MgSO_4$), and filtered. The yellow solid that was obtained after removal of the solvent was purified by column chromatography [SiO_2, 3:7 (v/v) DCM/EtOAc eluent], yielding *fac*-**9** (0.03 g, 58%) as a yellow solid. Anal. Calcd for $C_{75}H_{78}F_3IrN_6$: C, 68.62; H, 5.99; N, 6.40. Found: C, 68.37; H, 6.05; N, 6.30. ^1H NMR (600 MHz, CD_2Cl_2): δ 8.14 (3H, d, J = 10.5 Hz), 7.79 (3H, s), 7.72 (3H, dd, J = 8.3, 5.7 Hz), 7.45−7.38 (3H, m), 7.36−7.28 (6H, m), 6.99−6.89 (3H, m), 6.53 (3H, td, J = 8.7, 2.7 Hz), 6.44 (3H, d, J = 10.2 Hz), 4.18 (6H, d, J = 7.6 Hz), 2.05 (3H, dd, J = 12.3, 6.6 Hz), 1.43−1.14 (24H, m), 0.85 (18H, m). ^{19}F NMR (564 MHz, CD_2Cl_2): δ −114.2 (3F, s). HRMS (FTMS + ESI): calcd for $[C_{75}H_{78}F_3{}^{193}IrN_6 + H^+]$ 1313.5948, found 1313.5927.

Computational Data. All computations were conducted with the Gaussian 09 package.[35] The model geometries from various starting conformers were fully optimized with the B3LYP/3-21G*/LANL2DZ basis set. Using this functional and basis set, the TD-DFT data were obtained.

RESULTS AND DISCUSSION

Synthesis. The synthesis of ligand **6**, shown in Scheme 1, followed a literature precedent for other pyrido[4,3-*b*]indole derivatives[36] and proceeded in 32% overall yield. Ligand **6** incorporates a difluorophenyl substituent to shift the emission toward the blue portion of the spectrum. The *N*-2-ethylhexyl substituent was chosen to impart solubility to the final products. Ligand **6** was reacted with iridium(III) chloride under standard conditions[37,38] (step iv) for forming a bridged μ-dichloro diiridium C^N ligand complex **7**. This intermediate was reacted without further purification with a mixture of **6**, acetylacetone, and NEt_3 in ethylene glycol at 190 °C to give a yellow solid. Mass spectrometry and elemental analysis were consistent with homoleptic Ir(III) complex **8**. NMR spectra (Figure 1 and Figures S3 and S4 of the Supporting Information) clearly showed that the asymmetric *mer* isomer had been isolated: five peaks are present in the ^{19}F NMR spectrum, and the characteristically complex aromatic region is observed in the ^1H NMR spectrum. The X-ray crystal structure of *mer*-**8** is shown in Figure 2.

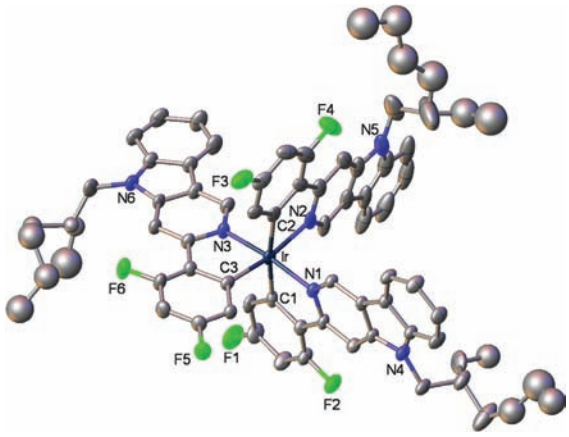

Figure 2. X-ray molecular structure of *mer*-**8** at 120 K, showing only one conformation of the disordered side chains. Thermal ellipsoids are drawn at the 50% probability level. Hydrogen atoms have been omitted for the sake of clarity.

Attempts to convert *mer*-**8** into *fac*-**8** using standard thermal conditions[11−15,21] were unsuccessful. Heating *mer*-**8** in glycerol at temperatures of ≤265 °C for 18 h resulted in quantitative recovery of *mer*-**8**. At higher temperatures (270−290 °C for 18 h), partial defluorination occurred and a mixture of unreacted *mer*-**8** and *fac*-**9** was obtained. Heating *mer*-**8** in glycerol at 290 °C for 72 h gave pure *fac*-**9** in 58% yield. No other complex could be isolated. The structure of *fac*-**9** was established by ^1H and ^{19}F NMR spectra, which showed the C_3 symmetry of the *fac* isomer, high-resolution mass spectrometry, and elemental analysis. It is clear from the ^1H and ^{19}F NMR spectra (Figures S7 and S8 of the Supporting Information) that the loss of fluorine is regiospecific for each ligand. In particular, the COSY spectrum (Figure S9 of the Supporting Information) shows three hydrogen environments on each ligand that possess no three-bond coupling to a neighboring hydrogen (one on the fluorophenyl ring and two on the pyridyl ring) (see the Supporting Information). This confirms that the fluorine at C4 is retained. If the fluorine at C6 had been retained, there would be only two hydrogen environments (those on the pyridyl ring) with no three-bond coupling. The preferential loss of the fluorine (as fluoride) from C6 rather than C4 of the phenyl rings of *mer*-**8** can be explained by the enhanced electrophilicity of C6, compared to that of C4, due to the electron-withdrawing pyridine ring at the *ortho* C1 position. The high thermal stability of *fac*-**8** (see below) provides evidence that defluorination occurs from the *mer* isomer, not the *fac* isomer of **8**, although the detailed mechanism is unclear.

Photoisomerization of *mer*-**8** was successfully achieved by irradiation of *mer*-**8** in degassed CD_2Cl_2 in an NMR tube with UV light (365 nm). The conversion to *fac*-**8** was quantitative as determined by ^1H and ^{19}F NMR analysis. Figure 1 shows the evolution of the ^{19}F NMR spectrum upon photolysis. This is consistent with a report by Thompson et al. of clean photochemical isomerization of *mer*-tris(4,6-difluorophenyl)-pyridinato-*N*,C^2-iridium(III) [*mer*-Ir(46dfppy)$_3$] to the *fac* isomer **10** (Chart 1), a reaction that could not be achieved thermally in refluxing glycerol.[21] De Cola et al. also reported the high thermal stability of *mer* isomers of fluorinated Ir(ppy)$_3$ systems: for example, only *mer*-tris[2-(3′,4′,6′-trifluorophenyl)-pyridinato]-*N*,C^2-iridium(III) [*mer*-Ir(F_3ppy)$_3$] was obtained at 250 °C.[24] No defluorinated products were reported in these studies.[21,24] It appears, therefore, to be a general feature that fluorinated *mer* cyclometalates do not isomerize as easily as nonfluorinated analogues. We assume that the *mer*-**8** to *fac*-**8** isomerism is a unimolecular process, based on literature precedents.[14]

The thermally induced defluorination of *mer*-**8** merits further discussion as fluorinated aryl groups are widely used to shift the emission of cyclometalated Ir complexes to the blue portion of the spectrum.[21−24] Holmes et al. noted that there may be drawbacks to this strategy as the high electronegativity of fluorine could make the ligands electrochemically reactive in OLEDs.[39] More recently, high-performance liquid chromatography coupled with mass spectrometry (HPLC−MS) showed

dx.doi.org/10.1021/ic201655n | *Inorg. Chem.* 2012, 51, 290−297

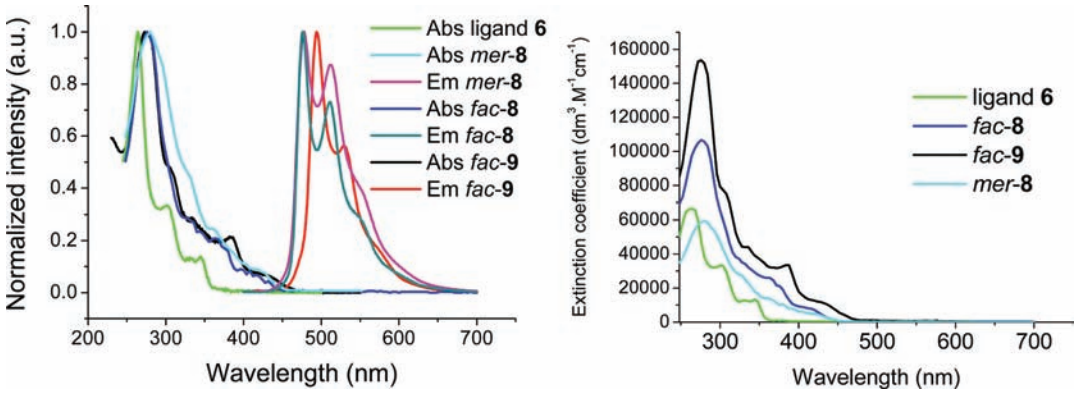

Figure 3. Normalized absorption and emission spectra (left) of ligand **6** and complexes *mer*-**8**, *fac*-**8**, and *fac*-**9**. Absorption spectra (right) with molar extinction coefficients. Spectra were recorded in a degassed dichloromethane solution.

Table 1. Photophysical and Solution Electrochemical Data

complex	λ_{max}^{abs} (nm)[a]	λ_{max}^{em} (nm)[a,b]	PLQY, Φ_{PL}[a,c]	τ_P (μs)[a,d]	τ_0 (μs)[e]	$E^{ox}_{1/2}$ (V)[f]
mer-**8**	278	477, 512	–	–	–	0.90
fac-**8**	280	476, 511	0.31	4.5	14.5	0.95
fac-**9**	272	494, 529	0.22	4.3	19.5	0.71

[a]Data obtained in a degassed dichloromethane solution at 20 °C. [b]Excitation wavelength of 380 nm. [c]Measured using an integrating sphere; estimated error of ±10%. [d]Estimated error of ±5%. [e]Calculated using the relationship $\tau_0 = \tau_P \times \Phi_T/\Phi_P$ and assuming $\Phi_T = 1$. [f]Redox data were obtained in a dichloromethane solution and are reported vs $FcMe_{10}/FcMe_{10}^+$ ($FcMe_{10}/FcMe_{10}^+ = -0.59$ V vs Fc/Fc^+).[46]

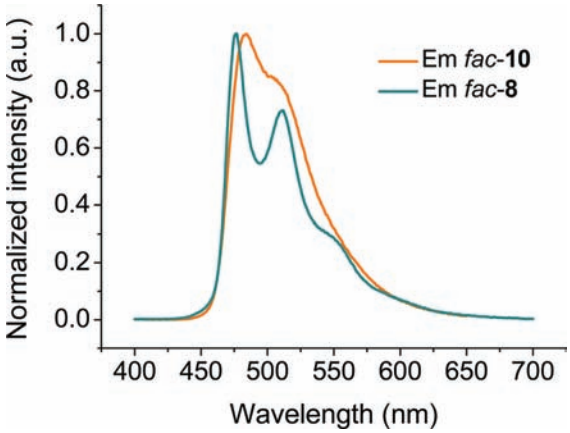

Figure 4. Normalized emission spectra of *fac*-**8** and *fac*-**10** in a degassed dichloromethane solution.

that the heteroleptic complex bis(4,6-difluorophenyl)-pyridinato-*N*,C^2-iridium(picolinate) (FIrpic), which is a standard sky-blue phosphor,[40,41] decomposes during the manufacture of OLED (i.e., vacuum sublimation) and operation of the device to give a complex mixture of defluorinated products.[42,43] In our work, we have isolated a single defluorinated product (*fac*-**9**) from a homoleptic complex (*mer*-**8**) under controlled thermal conditions. This observation establishes that defluorination may be a more general problem with Ir complexes containing multifluorinated ligands.

In contrast to *mer*-**8**, *fac*-**8** is thermally very stable. No decomposition was observed upon refluxing *fac*-**8** in glycerol at 290 °C for 48 h. However, *fac*-Ir(46dfppy)$_3$ **10**[21] (Chart 1) is unstable under these conditions: heating *fac*-**10** in glycerol at

Table 2. B3LYP/3-21G*/LANL2DZ TD-DFT Calculated Lowest-Energy Transitions from the Ground State to the Lowest Triplet States

compd	triplet state	excitation[a]	energy (eV) [λ (nm)]
1′	T_1	LUMO ← HOMO	2.63 (471)
	T_2	LUMO + 1 ← HOMO	2.65 (469)
	T_3	LUMO + 2 ← HOMO	2.67 (465)
2′	T_1	LUMO ← HOMO	2.53 (490)
	T_2	LUMO + 1 ← HOMO	2.57 (482)
	T_3	LUMO + 2 ← HOMO	2.57 (482)
mer-**8′**	T_1	LUMO + 2 ← HOMO	2.78 (446)
		LUMO ← HOMO	
	T_2	LUMO + 2 ← HOMO	2.82 (440)
		LUMO + 1 ← HOMO	
	T_3	LUMO ← HOMO − 1	2.85 (436)
fac-**8′**	T_1	LUMO ← HOMO	2.77 (447)
	T_2	LUMO + 1 ← HOMO	2.79 (445)
	T_3	LUMO + 2 ← HOMO	2.79 (445)
fac-**9′**	T_1	LUMO ← HOMO	2.62 (472)
	T_2	LUMO + 2 ← HOMO	2.65 (467)
	T_3	LUMO + 1 ← HOMO	2.65 (467)
11	T_1	LUMO ← HOMO	2.40 (516)
	T_2	LUMO + 1 ← HOMO	2.43 (510)
	T_3	LUMO + 2 ← HOMO	2.44 (509)
12	T_1	LUMO ← HOMO	2.26 (549)
	T_2	LUMO + 1 ← HOMO	2.27 (545)
		LUMO ← HOMO − 1	
	T_3	LUMO + 2 ← HOMO	2.27 (545)
		LUMO ← HOMO − 2	

[a]Dominant component(s).

290 °C for 2 h led to extensive decomposition to a multitude of products (TLC evidence) that could not be isolated. We note that Thompson et al. reported that *mer*-**10** did not isomerize when refluxed in glycerol for 24 h, which the authors ascribed to a large kinetic barrier that needed to be overcome for this derivative. It was not stated if any products were detected.[21] These results establish that the γ-carboline system of *fac*-**8** imparts additional thermal stability to the complexes, compared to the pyridyl analogue *fac*-**10**.

X-ray Crystal Structure of *mer*-8. The asymmetric unit comprises one molecule. The iridium atom adopts a *mer*-octahedral coordination (Figure 2) with three C^N-chelating ligands. In agreement with the rules of *trans* influence,[21] the Ir–N1 and Ir–N3 bonds (in *trans* positions with respect to each

dx.doi.org/10.1021/ic201655n | *Inorg. Chem.* 2012, 51, 290–297

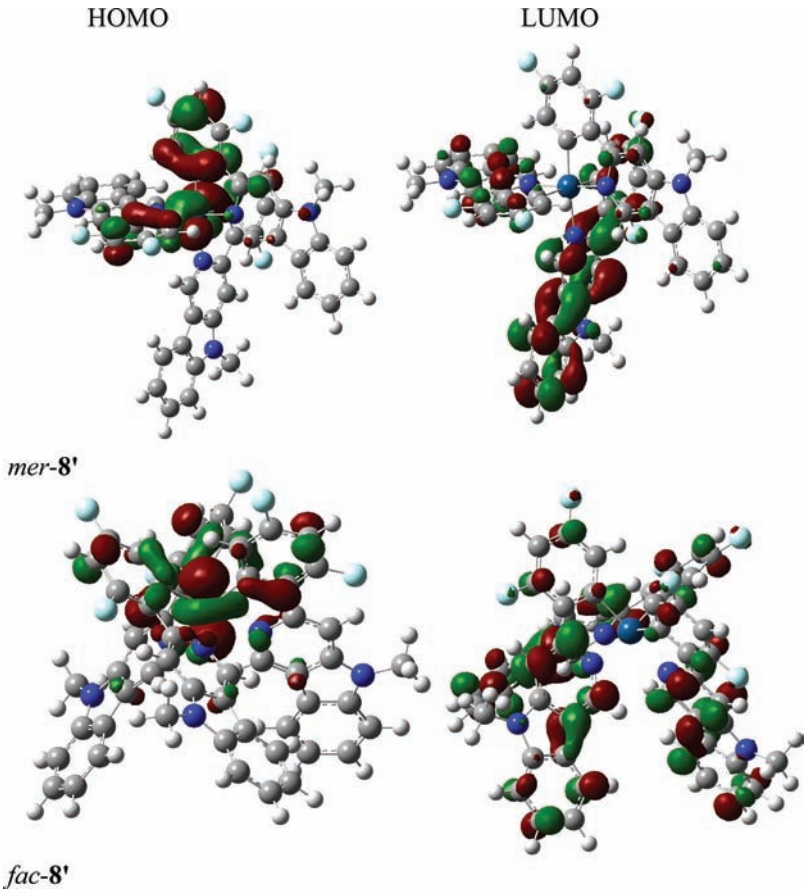

Figure 5. HOMO and LUMO orbital plots for *mer*-**8′** and *fac*-**8′** (C, gray; H, white; Ir, turquoise; N, blue; F, sky blue).

other) are shorter [2.065(4) and 2.050(4) Å, respectively] than the Ir−N2 bond [2.145(6) Å], which is *trans* to the 1.978(6) Å Ir−C3 bond, whereas the latter is shorter than Ir−C1 and Ir−C2 bonds [2.040(7) and 2.069(7) Å, respectively], which are *trans* to each other.

Photophysical and Electrochemical Properties. The absorption and emission spectra of *mer*-**8**, *fac*-**8**, and *fac*-**9** and the absorption spectrum of ligand **6** in an oxygen-free dichloromethane solution are shown in Figure 3, and the data are listed in Table 1. The complexes show strong absorption bands in the 250−300 nm region that are assigned[18] to ligand-centered $\pi-\pi^*$ transitions and closely resemble the absorption spectrum of the free ligand **6**. The complexes show absorption bands with lower extinction coefficients in the range of 350−450 nm that are ascribed to singlet and triplet metal-to-ligand charge-transfer (^{1}MLCT and ^{3}MLCT) states, following literature precedent[18] and the calculations of Hay.[44] The emission of the complexes is in the blue-green region. The following trends in this series of complexes can be seen. (i) The λ_{max}^{em} values for *mer*-**8** and *fac*-**8** are essentially the same, although for *mer*-**8** the lower-energy vibronic band is more intense relative to the analogous band for *fac*-**8**. This is a subtle difference, as seen previously,[24] whereas significant broadening of the emission is seen in the *mer* isomer for other *fac*−*mer* pairs.[21] (ii) The λ_{max}^{em} of *fac*-**9** is significantly red-shifted (by 18 nm, i.e., 770 cm^{-1}) compared to that of *fac*-**8** because of the loss of a fluorine substituent from each ligand in *fac*-**9**. The emission from *fac*-**9** is visibly greener compared to that of *mer*-**8** and *fac*-**8**. (iii) The λ_{max}^{em} of *fac*-**8** (476 nm in DCM) is blue-shifted compared to that of *fac*-**10** [484 nm (Figure 4)] (cf. *fac*-**10** λ_{max}^{em} values of 480 nm in chloroform[45] and 468 nm in 2-methyltetrahydrofuran[21]). The electron donating effect of the carboline nitrogen at position 4 of the pyridyl ring of *fac*-**8**, which should raise the LUMO and blue shift the emission,[12] apparently outweighs the effects of extending the π-system, which should red shift the emission.[28]

The photoluminescence quantum yield (PLQY) and lifetime data (observed and pure radiative) for *fac*-**8** and *fac*-**9** are listed in Table 1. These data could not be reliably obtained for *mer*-**8** because of its partial conversion to *fac*-**8** during the experiment, observed by changes in the emission spectrum. The observed lifetimes of *fac*-**8** and *fac*-**9** (τ_P = 4.5 and 4.3 μs, respectively) and the spectral profiles are indicative of phosphorescence from a mixture of ligand-centered and MLCT excited states. These lifetimes are relatively long compared to that of *fac*-Ir(ppy)$_3$ (1.9 μs in 2-methyltetrahydrofuran)[21] and those of *fac*-Ir(F$_3$-ppy)$_3$ and *fac*-Ir(F$_4$-ppy)$_3$ (1.6 and 2.3 μs, respectively, in degassed dichloromethane).[24]

The electrochemical properties of complexes *mer*-**8**, *fac*-**8**, and *fac*-**9** were examined by cyclic voltammetry in a dichloromethane solution. The complexes showed reversible oxidation waves assigned to the Ir(III)/Ir(IV) couple (Table 1). No additional ligand-centered oxidation waves were seen on scanning to 2.0 V. No reduction waves were observed on scanning between 0 and −2.0 V. *mer* isomers are generally easier to oxidize for reasons explained previously.[21] The lower oxidation potential of *mer*-**8** compared to that of *fac*-**8** ($\Delta E^{ox}_{1/2}$ = 50 mV) is consistent with data for other pairs of *mer* and *fac* isomers.[21,24] Similarly, as expected, the loss of a fluorine atom

dx.doi.org/10.1021/ic201655n | *Inorg. Chem.* 2012, 51, 290−297

from each ligand lowers the oxidation potential of *fac*-**9** by 240 mV compared to that of *fac*-**8**.

DFT Calculations. To guide our synthetic targets in this work, we conducted B3LYP/3-21G*/LANL2DZ density functional theory (DFT) calculations on *fac*-**1′**, *fac*-**2′**, and the isomeric ring systems *fac*-**11** and *fac*-**12** (Chart 2). To reduce computation time, the *N*-methyl analogues of *fac*-**1** and *fac*-**2** (*fac*-**1′** and *fac*-**2′**, respectively) were calculated. The calculations suggested that the $T_1 \leftarrow S_0$ transition of **2′** (2.53 eV) is similar in energy to that of **1′** (2.63 eV) and should, therefore, preserve the green emission observed for **1**,[29−31] whereas for isomeric systems **11** and **12**, the comparable transitions have lower energies (2.40 and 2.26 eV, respectively). These data and those for *mer*-**8′**, *fac*-**8′**, and *fac*-**9′** are listed in Table 2. It can be seen that attachment of fluorine atoms to the phenyl rings of the ligands increases the HOMO−LUMO gap, leading to the observed blue-shifted emission.

The HOMO and LUMO surfaces of *mer*-**8′** and *fac*-**8′** are shown in Figure 5. For both isomers, the HOMO is located on the iridium and difluorophenyl units. The LUMO is predominantly localized on one of the carboline ligands of *mer*-**8′**, whereas it is distributed equally among the three carboline ligands of *fac*-**8′**. The HOMO−LUMO surfaces for *fac*-**9′** (Figure S16 of the Supporting Information) are similar to those for *fac*-**8′**. These data are consistent with the HOMO−LUMO distributions in related $Ir(C^{\wedge}N)_3$ complexes.[21,44]

CONCLUSIONS

New homoleptic tris-cyclometalated $[Ir(C^{\wedge}N)_3]$ complexes have been synthesized and characterized using a range of techniques. *mer*-**8** can be cleanly isomerized to *fac*-**8** under photochemical conditions. However, under thermal conditions (heating at 290 °C in glycerol), an unusual regioselective defluorination reaction of *mer*-**8** occurs, yielding *fac*-**9** in 58% isolated yield. No decomposition was observed upon refluxing *fac*-**8** in glycerol at 290 °C for 48 h. The γ-carboline system of *fac*-**8** imparts high thermal stability to the complex, compared to that of the pyridyl analogue *fac*-**10**, which undergoes extensive decomposition upon being heated in glycerol at 290 °C for 2 h. The new complexes *mer*-**8**, *fac*-**8**, and *fac*-**9** are emitters of blue-green light (λ_{max}^{em} = 477, 476, and 494 nm, respectively), and their solution photophysical and electrochemical properties have been evaluated. The complexes are phosphorescent with triplet lifetimes for *fac*-**8** and *fac*-**9** of ∼4.5 μs at room temperature; the solution Φ_{PL} values were 0.31 and 0.22, respectively. There is broader significance in this work for the design of ligands and their use in phosphorescent complexes. (i) Fluorinated aromatic ligands are extensively used as components of blue phosphors for OLEDs.[21−27] Our results provide new evidence that multifluorinated ligands are not ideal because of their thermal instability in some complexes. This should provide added impetus for the development of blue phosphors with fewer[47] or no fluorine substituents.[28,48,49](ii) The improved thermal stability imparted by the γ-carboline moiety of *fac*-**8**, compared to pyridyl analogue *fac*-**10**, suggests that (hetero)carbazole derivatives should be exploited further as ligands for robust cyclometalated Ir complexes.

ASSOCIATED CONTENT

Supporting Information

Synthesis and characterization data for **3**−**6**; X-ray crystallographic data, including files in CIF format for *mer*-**8**; copies of NMR spectra of **7**, *mer*-**8**, *fac*-**8**, and *fac*-**9**; luminescence decay profiles of *fac*-**8** and *fac*-**9**; cyclic voltammograms of *mer*-**8**, *fac*-**8**, and *fac*-**9**; and computational data. This material is available free of charge via the Internet at http://pubs.acs.org.

AUTHOR INFORMATION

Corresponding Author

*E-mail: m.r.bryce@durham.ac.uk.

ACKNOWLEDGMENTS

We thank Durham University (Y.Z. and R.M.E.) and Thorn Lighting (Y.Z.) for funding. R.M.E. is funded by a Durham Doctoral Fellowship.

REFERENCES

(1) Lowry, M. S.; Bernhard, S. *Chem.—Eur. J.* **2006**, *12*, 7970−7977.
(2) Lo, K. K.-W.; Hui, W.-K.; Cheng, C.-K.; Tsang, K. H.-K.; Ng, D. C.-M.; Zhu, N.; Cheung, K.-K. *Coord. Chem. Rev.* **2005**, *249*, 1434−1450.
(3) Kakafi, Z. H. *Organic Electroluminescence*; CRC Press: New York, 2005.
(4) Müllen, K.; Scherf, U. *Organic Light-Emitting Devices*; Wiley-VCH: Weinheim, Germany, 2006.
(5) Li, Z.; Meng, H. *Organic Light-Emitting Materials and Devices*; CRC Press: Boca Raton, FL, 2006.
(6) Yersin, H., Ed. *Highly Efficient OLEDs with Phosphorescent Materials*; Wiley-VCH, Weinheim, Germany, 2008.
(7) Kamtekar, K. T.; Monkman, A. P.; Bryce, M. R. *Adv. Mater.* **2010**, *22*, 572−582.
(8) Holder, E.; Langeveld, B. M. W.; Schubert, U. S. *Adv. Mater.* **2005**, *17*, 1109−1121.
(9) Chou, P.-T.; Chi, Y. *Chem.—Eur. J.* **2007**, *13*, 380−395.
(10) Wong, W.-Y.; Ho, C.-L. *J. Mater. Chem.* **2009**, *19*, 4457−4482.
(11) Karatsu, T.; Nakamura, T.; Yagai, S.; Kitamura, A.; Yamaguchi, K.; Matsushima, Y.; Iwata, T.; Hori, Y.; Hagiwara, T. *Chem. Lett.* **2003**, *32*, 886−887.
(12) Laskar, I. R.; Hsu, S.-F.; Chen, T.-M. *Polyhedron* **2005**, *24*, 189−200.
(13) McDonald, A. R.; Lutz, M.; von Chrzanowski, L. S.; van Klink, G. P. M.; Spek, A. L.; van Koten, G. *Inorg. Chem.* **2008**, *47*, 6681−6691.
(14) Tsuchiya, K.; Ito, E.; Yagai, S.; Kitamura, A.; Karatsu, T. *Eur. J. Inorg. Chem.* **2009**, 2104−2109.
(15) Deaton, J. C.; Young, R. H.; Lenhard, J. R.; Rajeswaran, M.; Huo, S. *Inorg. Chem.* **2010**, *49*, 9151−9161.
(16) Baldo, M. A.; O'Brien, D. F.; You, Y.; Shoustikov, A.; Sibley, S.; Thompson, M. E.; Forrest, S. R. *Nature* **1998**, *395*, 151−154.
(17) Baldo, M. A.; Lamansky, S.; Burrows, P. E.; Thompson, M. E.; Forrest, S. R. *Appl. Phys. Lett.* **1999**, *75*, 4−6.
(18) Lamansky, S.; Djurovich, P.; Murphy, D.; Abdel-Razzaq, F.; Lee, H.-E.; Adachi, C.; Burrows, P. E.; Forrest, S. R.; Thompson, M. E. *J. Am. Chem. Soc.* **2001**, *123*, 4304−4312.
(19) Tsuboyama, A.; Iwawaki, H.; Furugori, M.; Mukaide, T.; Kamatani, J.; Igawa, S.; Moriyama, T.; Miura, S.; Takiguchi, T.; Okada, S.; Hoshino, M.; Ueno, K. *J. Am. Chem. Soc.* **2003**, *125*, 12971−12979.
(20) Zhou, G.; Ho, C.-L.; Wong, W.-Y.; Wang, Q.; Ma, D.; Wang, L.; Lin, Z.; Marder, T. B.; Beeby, A. *Adv. Funct. Mater.* **2008**, *18*, 499−511.
(21) Tamayo, A. B.; Alleyne, B. D.; Djurovich, P. I.; Lamansky, S.; Tsyba, I.; Ho, N. N.; Bau, R.; Thompson, M. E. *J. Am. Chem. Soc.* **2003**, *125*, 7377−7387.
(22) Coppo, P.; Plummer, E. A.; De Cola, L. *Chem. Commun.* **2004**, 1774−1775.
(23) Dedeian, K.; Shi, J.; Shepherd, N.; Forsythe, E.; Morton, D. C. *Inorg. Chem.* **2005**, *44*, 4445−4447.
(24) Ragni, R.; Plummer, E. A.; Brunner, K.; Hofstraat, J. W.; Babudri, F.; Farinola, G. M.; Naso, F.; De Cola, L. *J. Mater. Chem.* **2006**, *16*, 1161−1170.

(25) Takizawa, S.; Echizen, H.; Nishida, J.; Tsuzuki, T.; Tokito, S.; Yamashita, Y. *Chem. Lett.* **2006**, *35*, 748−749.
(26) Wu, L.-L.; Yang, C.-H.; Sun, I.-W.; Chu, S.-Y.; Kao, P.-C.; Huang, H.-H. *Organometallics* **2007**, *26*, 2017−2023.
(27) Seo, H.-J.; Yoo, K.-M.; Song, M.; Park, J. S.; Jin, S.-H.; Kim, Y. I.; Kim, J.-J. *Org. Electron.* **2010**, *11*, 564−572.
(28) Sajoto, T.; Djurovich, P. I.; Tamayo, A.; Yousufuddin, M.; Bau, R.; Thompson, M. E. *Inorg. Chem.* **2005**, *44*, 7992−8003.
(29) Bettington, S.; Tavasli, M.; Bryce, M. R.; Beeby, A.; Al-Attar, H.; Monkman, A. P. *Chem.—Eur. J.* **2007**, *13*, 1423−1431.
(30) Al-Attar, H. A.; Griffiths, G. C.; Moore, T. N.; Tavasli, M.; Fox, M. A.; Bryce, M. R.; Monkman, A. P. *Adv. Funct. Mater.* **2011**, *21*, 2376−2382.
(31) Ho, C.-L.; Wang, Q.; Lam, C.-S.; Wong, W.-Y.; Ma, D.; Wang, L.; Gao, Z.-Q.; Chen, C.-H.; Cheah, K.-W.; Lin, Z. *Chem.—Asian J.* **2009**, *4*, 89−103.
(32) Porrés, L.; Holland, A.; Pålsson, L.-O.; Monkman, A. P.; Kemp, C.; Beeby, A. *J. Fluoresc.* **2006**, *16*, 267−272.
(33) Sheldrick, G. M. *Acta Crystallogr.* **2008**, *A64*, 112−122.
(34) Dolomanov, O. V.; Bourhis, L. J.; Gildea, R. J.; Howard, J. A. K.; Puschmann, H. *J. Appl. Crystallogr.* **2009**, *42*, 339−341.
(35) Frisch, M. J.; Trucks, G. W.; Schlegel, H. B.; Scuseria, G. E.; Robb, M. A.; Cheeseman, J. R.; Scalmani, G.; Barone, V.; Mennucci, B.; Petersson, G. A.; Nakatsuji, H.; Caricato, M.; Li, X.; Hratchian, H. P.; Izmaylov, A. F.; Bloino, J.; Zheng, G.; Sonnenberg, J. L.; Hada, M.; Ehara, M.; Toyota, K.; Fukuda, R.; Hasegawa, J.; Ishida, M.; Nakajima, T.; Honda, Y.; Kitao, O.; Nakai, H.; Vreven, T.; Montgomery, J. A., Jr.; Peralta, J. E.; Ogliaro, F.; Bearpark, M.; Heyd, J. J.; Brothers, E.; Kudin, K. N.; Staroverov, V. N.; Kobayashi, R.; Normand, J.; Raghavachari, K.; Rendell, A.; Burant, J. C.; Iyengar, S. S.; Tomasi, J.; Cossi, M.; Rega, N.; Millam, J. M.; Klene, M.; Knox, J. E.; Cross, J. B.; Bakken, V.; Adamo, C.; Jaramillo, J.; Gomperts, R.; Stratmann, R. E.; Yazyev, O.; Austin, A. J.; Cammi, R.; Pomelli, C.; Ochterski, J. W.; Martin, R. L.; Morokuma, K.; Zakrzewski, V. G.; Voth, G. A.; Salvador, P.; Dannenberg, J. J.; Dapprich, S.; Daniels, A. D.; Farkas, O.; Foresman, J. B.; Ortiz, J. V.; Cioslowski, J.; Fox, D. J. *Gaussian 09*, revision A.02; Gaussian, Inc.: Wallingford, CT, 2009.
(36) Zhang, H.; Larock, R. C. *J. Org. Chem.* **2002**, *67*, 9318−9330.
(37) Nonoyama, M. *Bull. Chem. Soc. Jpn.* **1974**, *47*, 767−768.
(38) Sprouse, S.; King, K. A.; Spellane, P. J.; Watts, R. J. *J. Am. Chem. Soc.* **1984**, *106*, 6647−6653.
(39) Holmes, R. J.; Forrest, S. R.; Sajoto, T.; Tamayo, A.; Djurovich, P. I.; Thompson, M. E.; Brooks, J.; Tung, Y.-J.; D'Andrade, B. W.; Weaver, M. S.; Kwong, R. C.; Brown, J. J. *Appl. Phys. Lett.* **2005**, *87*, 243507.
(40) Adachi, C.; Kwong, R. C.; Djurovich, P.; Adamovich, V.; Baldo, M. A.; Thompson, M. E.; Forrest, S. R. *Appl. Phys. Lett.* **2001**, *79*, 2082−2084.
(41) Li, J.; Djurovich, P. I.; Alleyne, B. D.; Yousufuddin, M.; Ho, N. N.; Thomas, J. C.; Peters, J. C.; Bau, R.; Thompson, M. E. *Inorg. Chem.* **2005**, *44*, 1713−1727.
(42) Sivasubramaniam, V.; Brodkorb, F.; Hanning, S.; Loebl, H. P.; van Elsbergen, V.; Boerner, H.; Scherf, U.; Kreyenschmidt, M. *Cent. Eur. J. Chem.* **2009**, *7*, 836−845.
(43) Sivasubramaniam, V.; Brodkorb, F.; Hanning, S.; Loebl, H. P.; van Elsbergen, V.; Boerner, H.; Scherf, U.; Kreyenschmidt, M. *J. Fluorine Chem.* **2009**, *130*, 640−649.
(44) Hay, P. J. *J. Phys. Chem. A* **2002**, *106*, 1634−1641.
(45) http://www.sigmaaldrich.com/etc/medialib/docs/Aldrich/Bulletin/al_uv-vis_682594.Par.0001.File.tmp/al_uv-vis_682594.pdf.
(46) Connelly, N. G.; Creiger, W. E. *Chem. Rev.* **1996**, *96*, 877−910.
(47) Khozhevnikov, V. N.; Dahms, K.; Bryce, M. R. *J. Org. Chem.* **2011**, *76*, 5143−5148.
(48) Yeh, Y.-S.; Cheng, Y.-M.; Chou, P.-T.; Lee, G.-H.; Yang, C.-H.; Chi, Y.; Shu, C.-F.; Wang, C.-H. *ChemPhysChem* **2006**, *7*, 2294−2297.
(49) Lin, C.-H.; Chang, Y.-Y.; Hung, J.-Y.; Lin, C.-Y.; Chi, Y.; Chung, M.-W.; Lin, C.-L.; Chou, P.-T.; Lee, G.-H.; Chang, C.-H.; Lin, W.-C. *Angew. Chem., Int. Ed.* **2011**, *50*, 3182−3186.